Preview Model Predictive Control for Hypersonic Flight Vehicles

Zhuorui Liu, Weiqiang Tang*, Xiaoli Huang and Zhengxiang Yang

School of Automation and Electrical Engineering, Lanzhou University of Technology, Lanzhou, Gansu 730050, China

Abstract: Excellent maneuverability is one of the key factors in ensuring the successful completion of missions for hypersonic vehicles. Therefore, to address the tracking control problem for hypersonic vehicles, a novel composite control method is proposed by integrating preview control with model predictive control. Based on the introduced nonlinear aircraft model, linearization is performed using small-perturbation theory in preparation for subsequent controller design. Furthermore, building upon the discretized model, a preview controller and a model predictive controller are designed separately, and are subsequently integrated to finalize the design of the control system. The designed control system achieves good tracking of both velocity and altitude while satisfying all system constraints. Compared with the conventional model predictive control method, the proposed one demonstrates improved dynamic performance while requiring less control effort. For velocity tracking, throttle setting, and elevator deflection angle, the maximum values of the PMPC system are approximately 77.65%, 92.45%, and 65.48% of those of the MPC system, respectively. This fully validates the necessity of introducing preview control as a feedforward compensation and opens new avenues for high-performance control of hypersonic vehicles.

Keywords: Hypersonic vehicles, maneuvering, preview control, model predictive control, composite control, longitudinal tracking.

1. INTRODUCTION

As an aircraft operating in near-space, hypersonic vehicles demonstrate significant value in both military and civilian domains, particularly in areas such as long-range transportation, reconnaissance, and strike operations [1, 2]. These significant values have attracted considerable attention from scientists and engineers, sparking a global research boom in hypersonic vehicles. However, the unique aerodynamic shape, integrated engine-airframe design, and complex flight environment of hypersonic vehicles endow them with stronger nonlinearity, coupling, and uncertainty compared to conventional aircraft, posing unprecedented challenges for the design of control systems.

Given the dynamic characteristics of hypersonic vehicles, a wide range of control methods have been employed in the design of their control systems, such as feedback linearization, adaptive control, sliding mode control, and fuzzy control [3, 4]. Control systems designed based on feedback linearization typically require further enhancement of their robustness. Adaptive or sliding mode control systems exhibit strong robustness due to their inherent unique mechanisms, thereby ensuring effective control performance. The intelligent control systems for hypersonic vehicles achieve further performance enhancement due to their powerful learning capability. While these methods have achieved satisfactory control performance to some extent, none of them take the system constraints into account. It is known that all physical systems are subject to constraints. If these constraints are not satisfied, the actual performance of the system can be compromised or may even lead to system instability [5, 6].

Model predictive control (MPC) provides a receding-horizon optimization framework that can explicitly handle multivariable dynamics and hard constraints. MPC predicts future outputs using a model and computes a control sequence by solving an online constrained optimization problem [7, 8]. Due to its ability to pursue optimality while satisfying system constraints, MPC has gained considerable favor in the control of hypersonic vehicles [6, 9, 10]. Research shows that MPC systems also exhibit strong robustness, as they employ a rolling optimization strategy [11, 12]. As is well known, hypersonic vehicles frequently perform maneuvering flight to accomplish missions or avoid risks. In hypersonic vehicle MPC systems, maneuvering commands often take the form of step signals. To rapidly eliminate tracking errors, substantial control actions are required, which may degrade the system's dynamic performance and consequently reduce flight quality.

Preview control (PC) explicitly utilizes known future reference and/or disturbance information to generate anticipated feedforward actions, thereby reducing phase lag and improving system dynamic performance [13, 14]. Like conventional feedback control, PC

*Address correspondence to this author at the School of Automation and Electrical Engineering, Lanzhou University of Technology, Lanzhou, Gansu 730050, China; E-mail: twqzjh@163.com

© Copyright: *Journal of Intelligent Aeronautical Systems and Sustainable Flight Technologies 2025*

imposes stringent requirements on model accuracy, presenting a key limitation in real-world implementation. To exploit the complementary strengths of MPC and PC, a composite control strategy based on the integration of MPC and PC is proposed. The offline preview feedforward compensator utilizes future references and known disturbance information to enhance dynamic performance, while the online MPC system suppresses uncertainties, thereby improving the overall system performance.

The rest of this study is structured as follows. Section 2 describes the vehicle model and the composite controller design is presented in Section 3. The results and analysis are presented in Section 4, and the conclusion is provided in Section 5.

2. MATHEMATICAL MODEL OF A HYPERSONIC VEHICLE AND ITS LINEARIZATION

2.1. Mathematical Model of a Hypersonic Vehicle

Assuming constant the mass, center of mass, and structural configuration during flight, the longitudinal dynamics of the hypersonic vehicle can be expressed as [6]

$$\dot{V} = \frac{T\cos\alpha - D}{m} - g\sin\gamma \tag{1}$$

$$\dot{\gamma} = \frac{T\sin\alpha + L}{mV} - \frac{g\cos\gamma}{V} \tag{2}$$

$$\dot{h} = V\sin\gamma \tag{3}$$

$$\dot{\alpha} = q - \dot{\gamma} \tag{4}$$

$$\dot{q} = \frac{M_z}{I_{zz}} \tag{5}$$

where V denotes the velocity, h denotes the altitude, γ denotes the flight path angle, α denotes the angle of attack, q denotes the pitch rate. m, g, T, D, M_z, I_{zz} denote the vehicle mass, gravitational acceleration, thrust, drag, pitching moment, and pitch moment of inertia, respectively. The expressions for the lift L, drag D, thrust T, and pitching moment M_z are given by

$$L = \frac{1}{2}\rho V^2 S C_L \tag{6}$$

$$D = \frac{1}{2}\rho V^2 S C_D \tag{7}$$

$$T = \frac{1}{2}\rho V^2 S C_T \tag{8}$$

$$M_z = \frac{1}{2}\rho V^2 S\bar{c}\left[C_M(\alpha) + C_M(\delta) + C_M(q)\right] \tag{9}$$

$$\begin{cases} C_L = 0.6203\alpha \\ C_D = 0.6450\alpha^2 + 0.0043378\alpha + 0.003772 \\ C_T = \begin{cases} 0.02876\eta, \eta < 1 \\ 0.0224 + 0.0036\eta, \eta \geq 1 \end{cases} \\ C_M(\alpha) = -0.035\alpha^2 + 0.036617\alpha + 5.3261\times 10^{-6} \\ C_M(\delta) = c_e(\delta - \alpha) \\ C_M(q) = \dfrac{\bar{c}}{2V} q(-6.796\alpha^2 + 0.3015\alpha - 0.2289) \end{cases} \tag{10}$$

It should be noted that the above coefficient expressions are valid under a trimmed cruise condition [15], i.e., $M = 15$, $V = 15060\text{ft/s}$, $h = 110000\text{ft}$, $\gamma = 0\text{deg}$, $q = 0\text{deg/s}$. Some other physical parameters of the vehicle are provided in Table **1**. Additionally, the propulsion system can be described by the following second-order system:

$$\ddot{\eta} = -2\varsigma\omega_n\dot{\eta} - \omega_n^2\eta + \omega_n^2\eta_c \tag{11}$$

where η denotes the throttle setting, ς denotes the damping, and ω_n denotes the frequency.

2.2. Model Linearization

As stated in 2.1, the vehicle dynamics are strongly nonlinear, which is detrimental to the control system design synthesis based on linear theory. Therefore, the model is linearized at a trim point using small-perturbation theory [14, 15]. The state vector is defined

Table 1: Parameter List

Param	Value/Unit	Param	Value/Unit
$\bar{c}$	$80/\text{ft}$	I_{zz}	$7\times10^6/\text{slug}\cdot\text{ft}^2$
m	$9375/\text{slugs}$	S	$3603/\text{ft}^2$
c_e	$0.0292/\text{rad}^{-1}$	ρ	0.24325×10^{-4}

as $x=\left[V,h,\gamma,\alpha,q\right]^T$. Let the trim state be $x_0=\left[V_0,h_0,\gamma_0,\alpha_0,q_0\right]^T$, and the corresponding trim control input is $u_0=\left[\eta_0,\delta_0\right]^T$. Define the perturbation state vector as $\Delta x=\left[\Delta V,\Delta h,\Delta\gamma,\Delta\alpha,\Delta q\right]^T$, and the perturbation control input as $\Delta u=\left[\Delta\eta,\Delta\delta\right]^T$, respectively.

Linearization via a first-order Taylor series expansion of equations (1)-(5) about the trim point, while neglecting higher-order terms, gives the following continuous-time linear state-space model:

$$\Delta\dot{x}=A\Delta x+B\Delta u \tag{12}$$

$$\Delta y=C\Delta x \tag{13}$$

where A, B, C are the relevant matrices. Considering a trim condition $V_{\text{trim}}=15060\text{ft}\cdot\text{s}^{-1}$, $\gamma_{\text{trim}}=0\text{rad}$, $h_{\text{trim}}=110000\text{ft}$, $\alpha_{\text{trim}}=0.0312\text{rad}$, $q_{\text{trim}}=0\text{rad}\cdot\text{s}^{-1}$, $\delta_{\text{trim}}=-0.0069\text{rad}$, the model is linearized as

$$\Delta\dot{x}=A_0\Delta x+B_0\Delta u \tag{14}$$

$$\Delta y=C_0\Delta x \tag{15}$$

with

$$A_0=\begin{bmatrix} 0 & -3.1478\times10 & 0 & -4.7455\times10 & 0 \\ 2.7759\times10^{-7} & 0 & 0 & 4.3985\times10^{-2} & 0 \\ 0 & 1.5060\times10^{4} & 0 & 0 & 0 \\ -2.7759\times10^{-7} & 0 & 0 & -4.3985\times10^{-2} & 1 \\ 0 & 0 & 0 & 5.9418\times10^{-1} & -6.8216\times10^{-2} \end{bmatrix}$$

$$B_0=\begin{bmatrix} 2.7296\times10 & 0 \\ 5.6617\times10^{-7} & 0 \\ 0 & 0 \\ -5.6617\times10^{-7} & 0 \\ 0 & 3.3167 \end{bmatrix},\quad C_0=\begin{bmatrix} 1 & 0 & 0 & 0 & 0 \\ 0 & 0 & 1 & 0 & 0 \end{bmatrix}.$$

Furthermore, system (14, 15) can be discretized as

$$x\left(k+1\right)=A^*x\left(k\right)+B^*u\left(k\right) \tag{16}$$

where $A^*=e^{AT_s}$, $B^*=B\int_0^{T_s}e^{A\tau}\,d\tau$, T_s is the sampling period.

3. PREVIEW MODEL PREDICTIVE CONTROLLER DESIGN

This section develops a scheme by integrating preview feedforward compensation with constrained MPC. the proposed controller consists of an offline preview feedforward compensator and an online receding-horizon optimization module. The preview compensator uses available future reference and preview able disturbance information to generate $u_{\text{pre}}(k)$, while the MPC module computes a corrective input $u_{\text{mpc}}(k)$ based on feedback to satisfy hard constraints. The implemented control input is the superposition $u(k)=u_{\text{pre}}(k)+u_{\text{mpc}}(k)$.

3.1. Controller Design Process

A finite-horizon preview feedforward signal can be written as a linear combination of future reference and preview able disturbance signals:

$$u_{\text{pre}}(k)=\sum_{j=1}^{M_R}F_R(j)R(k+j)+\sum_{j=0}^{M_d}F_d(j)d(k+j) \tag{17}$$

The preview gains F_R and F_d can be computed offline (from a standard optimal preview-control synthesis). Therefore, once the future reference $R(k+j)$ and disturbance $d(k+j)$ are available, $u_{\text{pre}}(k)$ can be generated in real time. Here, the $d(k+j)$ can be estimated using an observer. Propagating the plant model with $u_{\text{pre}}(k)$ yields the corresponding preview-induced output $y_{\text{pre}}(k)$ as in Eq. (18).

$$y_{\text{pre}}(k)=Cx_{\text{pre}}(k) \tag{18}$$

Let H_p and H_u denote the prediction and control horizons, respectively ($H_u \le H_p$). In conventional MPC, the stacked output prediction can be written in the compact form $\boldsymbol{Y}(k)=\Xi x(k)+\Theta\boldsymbol{U}(k)$, where Ξ and Θ are built from the discrete-time state-space model. With the preview-induced output vector $\boldsymbol{Y}_{\text{pre}}(k)$, the PMPC prediction model is given by Eq. (19).

$$\boldsymbol{Y}_M(k)=\boldsymbol{Y}(k)+\boldsymbol{Y}_{pre}(k)=\Xi x(k)+\Theta\boldsymbol{U}(k)+\boldsymbol{Y}_{pre}(k) \tag{19}$$

with

$$\boldsymbol{Y}_M(k)=\begin{bmatrix} y_M(k+1\,|\,k) \\ \vdots \\ y_M(k+H_p\,|\,k) \end{bmatrix},\qquad \boldsymbol{Y}(k)=\begin{bmatrix} y(k+1\,|\,k) \\ \vdots \\ y(k+H_p\,|\,k) \end{bmatrix},$$

$$\boldsymbol{Y}_{pre}(k)=\begin{bmatrix} y_{pre}(k\,|\,k) \\ \vdots \\ y_{pre}(k+H_p-1\,|\,k) \end{bmatrix}.$$

At each sampling instant k, a prediction error is computed between the measured output $y(k)$ and the one-step-ahead model prediction $y_{\text{pre}}(k|k-1)$ obtained at the previous sampling instant. Assuming that the mismatch is approximately constant over the short horizon, this offset is added to the future predictions, leading to the correction term defined in Eq. (20).

$$e_M(k+\tau|k) = y_p(k) - y_M(k) \tag{20}$$

where $y_p(k)$ denotes the measured (plant) output, and $y_M(k)$ denotes the model prediction of $y_p(k)$ computed at the previous step ($y_M(k) = y_{\text{pre}}(k|k-1)$).

Following the receding-horizon principle, at each time k the PMPC computes an optimal control sequence by minimizing a quadratic objective that penalizes the corrected output tracking error and control effort, as in Eq. (21).

$$\begin{aligned} h_M(k) = &\sum_{\tau=1}^{H_p} \left\| y_M(k+\tau|k) + e_M(k+\tau|k) - r(k+\tau) \right\|_{Q(\tau)}^2 \\ &+ \sum_{\tau=0}^{H_u-1} \left\| u(k+\tau|k) \right\|_{R(\tau)}^2 \end{aligned} \tag{21}$$

where Q and R are weighting matrices, and $r(k+\tau)$ is the previewed reference trajectory. The same weights are used for both output channels (velocity and altitude) unless otherwise stated. By stacking the predicted outputs, reference signals, and correction terms, the objective can be rewritten in a compact form as (22), which is quadratic in the stacked control vector $u(k)$.

$$h_M(k) = \left\| \boldsymbol{U}(k) \right\|_R^2 + \left\| \boldsymbol{Y}_M(k) + \boldsymbol{E}_M(k) - \boldsymbol{\Upsilon}(k) \right\|_{\boldsymbol{Q}}^2 \tag{22}$$

where $\boldsymbol{E}_M(k) = \begin{bmatrix} e_M^{\mathrm{T}}(k+1|k) & \cdots & e_M^{\mathrm{T}}(k+H_p|k) \end{bmatrix}^{\mathrm{T}}$,

$\boldsymbol{U}(k) = \begin{bmatrix} u^{\mathrm{T}}(k+1|k) & \cdots & u^{\mathrm{T}}(k+H_u|k) \end{bmatrix}^{\mathrm{T}}$,

$\boldsymbol{\Upsilon}(k) = \begin{bmatrix} r^{\mathrm{T}}(k+1|k) & \cdots & r^{\mathrm{T}}(k+H_p|k) \end{bmatrix}^{\mathrm{T}}$.

For convenience, define the variable $\boldsymbol{\varpi}_M(k)$ in Eq. (23), which collects all known terms (current state, reference, prediction correction, and the preview-induced output).

$$\boldsymbol{\varpi}_M(k) = \boldsymbol{\Upsilon}(k) - \boldsymbol{\Xi} x(k) - \boldsymbol{E}_M(k) - \boldsymbol{Y}_{pre}(k) \tag{23}$$

So, the (22) can be further simplified as

$$\begin{aligned} h_M(k) &= \left\| \Theta \boldsymbol{U}(k) - \boldsymbol{\varpi}_M(k) \right\|_{\boldsymbol{Q}}^2 + \left\| \boldsymbol{U}(k) \right\|_{\boldsymbol{R}}^2 \\ &= \boldsymbol{\varpi}_M{}^T(k) \boldsymbol{Q} \boldsymbol{\varpi}_M(k) - \boldsymbol{U}^T(k) \boldsymbol{\wp}_M + \boldsymbol{U}^T(k) \hbar \boldsymbol{U}(k) \end{aligned} \tag{24}$$

Note that $\boldsymbol{\varpi}_M{}^T(k) \boldsymbol{Q} \boldsymbol{\varpi}_M(k)$ in (24) is constant with respect to $\boldsymbol{U}(k)$. Therefore, differentiating the quadratic objective yields the gradient in Eq. (25).

$$\nabla_{U(k)} h = -\boldsymbol{\wp}_M + 2\hbar \boldsymbol{U}(k) \tag{25}$$

If no constraints are imposed, setting the gradient to zero gives the closed-form solution in Eq. (26). In the constrained case considered here, the magnitude and rate limits of control input are enforced, and the optimization is solved as a convex QP with linear inequality constraints at each sampling instant, more details can be found in the references.

$$\boldsymbol{U}(k) = \frac{1}{2} \hbar^{-1} \boldsymbol{\wp}_M \tag{26}$$

3.2. Implementation Procedure

(1) Offline preview design: Select preview-control weights and preview lengths (M_R and M_d) based on the available future reference and disturbance information, and compute the preview gains F_R and F_d.

(2) MPC parameter selection: Choose the sampling period T_s, prediction horizon H_p, control horizon H_u ($H_u \le H_p$), and the MPC weighting matrices Q and R, specify actuator magnitude and rate constraints.

(3) Preview generation: At each time k, compute $u_{\text{pre}}(k)$ using Eq. (17) from the available future reference and preview able disturbance data, and propagate the model to obtain $y_{\text{pre}}(k)$.

(4) Online QP optimization: Measure $y(k)$ or estimate $x(k)$, compute the prediction correction term using Eq. (20), build the PMPC prediction model in Eq. (19), and solve the constrained QP corresponding to Eq. (22) to obtain the optimal corrective sequence $u^*(k)$.

(5) Apply the first control move: $u_{\text{mpc}}(k)$ is taken as the first element of $u^*(k)$, and the applied input is $u(k) = u_{\text{pre}}(k) + u_{\text{mpc}}(k)$.

(6) Repeat Steps (3)-(5) at the next sampling instant (receding horizon).

Remark 1. The preview information utilized in the controller design includes both the reference output and disturbance signals. Generally, the former can be obtained via navigation systems, while the latter is typically acquired by first estimating the current value using an observer, followed by extrapolation techniques to derive estimated values for a future time period. Although the future estimates may contain errors, the rolling optimization mechanism of MPC effectively mitigates the impact of such inaccuracies.

4. RESULTS AND ANALYSIS

It is assumed that the aircraft conducts maneuvering flight under a cruise condition, and the control parameters are follows: $T_S = 0.001\text{s}$, $H_p = 100$, $H_u = 20$. The constraints are $\Delta\eta \le 0.1$, $0 \le \eta \le 3$, $\Delta\delta \le 3^o$, $-15^o \le \delta \le 15^o$. The weighting matrices in the prediction stage are: $Q = 0.001 \times \text{diag}(\text{ones}(1, 2 \times H_p))$, $R = 2 \times \text{diag}(\text{ones}(1, 2 \times H_u))$. It should be noted that the selection of the above control parameters was determined through a trial-and-error approach. Alternatively, sensitivity analysis can be performed on these parameters, and the selection can be made based on the analysis results. Furthermore, building on sensitivity analysis, optimization methods can be employed to determine the selection of key parameters. Additionally, regarding the determination of constraints, previous studies have shown that such a configuration is reasonable [6].

4.1. Validation of Effectiveness

Figures **2-5** illustrate the control performance of the proposed PMPC method for the hypersonic vehicle. In Figure **2**, the dashed line denotes the desired velocity, while the solid line denotes the actual one. It can be observed from Figure **2** that the velocity first decreases, then gradually increases, reaching the reference value within 15s with no overshoot. In Figure **3**, the dashed line denotes the reference signal and the solid line denotes the actual altitude. Likewise, it can be seen from Figure **3** that the altitude settles within 10 s with slight overshoot. However, the overshoot is almost negligible. Figures **4** and **5** depict the control input variables, namely the throttle setting and the control-surface deflection, respectively. As shown in Figures **4** and **5**, the throttle setting stabilizes within 15 s, and the control-surface deflection stabilizes in approximately 5 s. Moreover, all these control variables remain within

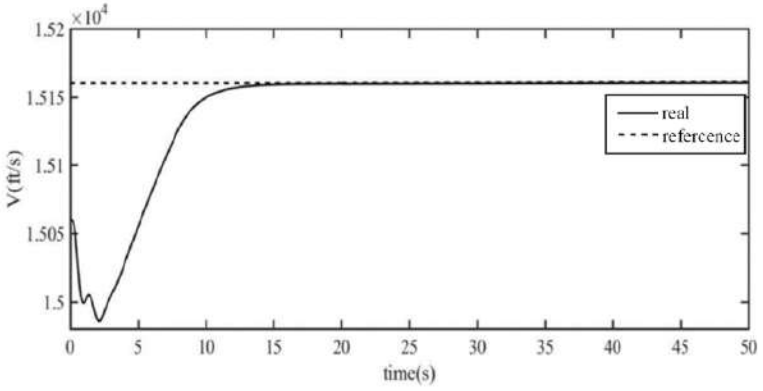

Figure 1: Velocity response under PMPC.

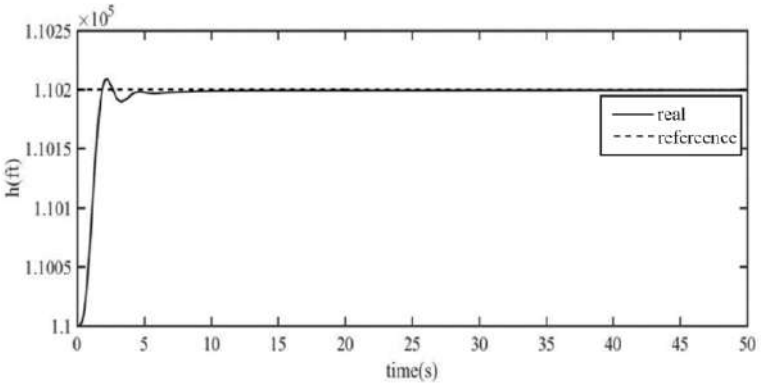

Figure 2: Altitude response under PMPC.

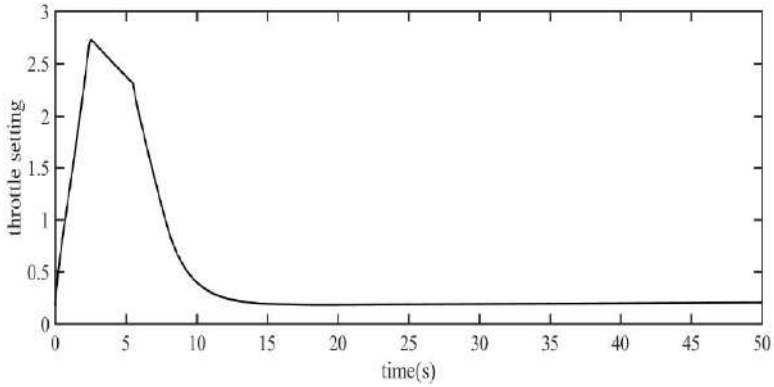

Figure 3: Throttle setting command under PMPC.

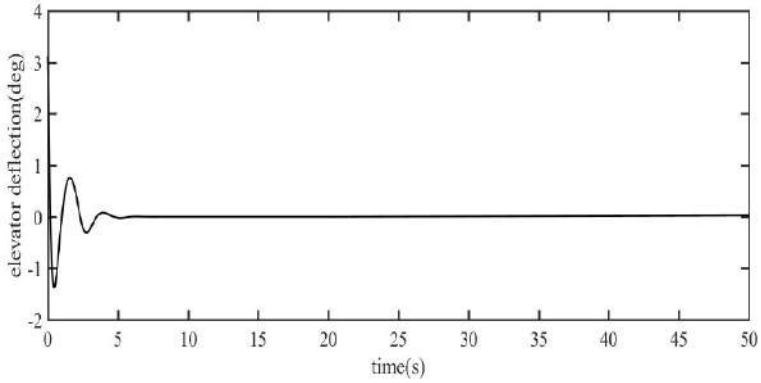

Figure 4: Control-surface deflection under PMPC.

the specified constraints. The above results demonstrate that the designed PMPC system achieves satisfactory tracking performance for the vehicle and validate the effectiveness of the proposed PMPC method.

4.2. Comparative Results and Analysis

To highlight the advantages of the proposed method, it is compared with conventional MPC, with the results shown in Figures **5-8**. In Figure **5**, the dashed line represents the velocity response under MPC, whereas the solid line represents the response under PMPC. As shown in Figure **5**, Both methods achieve satisfactory speed tracking performance, and their regulation processes are largely identical. However, the velocity reduction under PMPC is less than that under MPC, which is mainly due to the compensation effect of preview control. Unlike the velocity tracking, the altitude tracking performance is nearly identical under both methods, as shown Figure **6**, indicating that the feedforward compensation has a negligible effect on height tracking. For the throttle setting, as shown in Figure **7**, the required control effort under PMPC is lower during the dynamic phase, which is beneficial for enhancing the regulation capability of vehicles. Similar

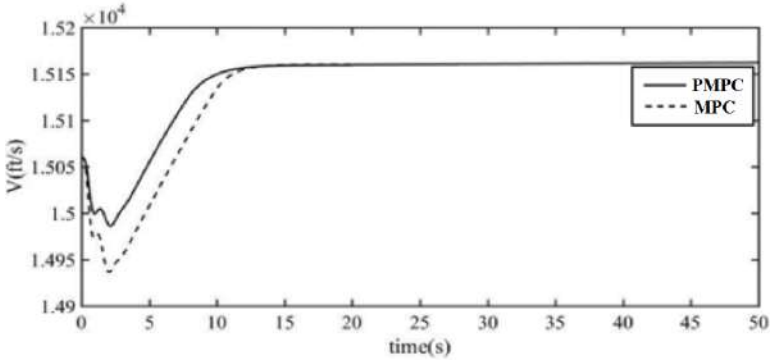

Figure 5: Velocity response comparison.

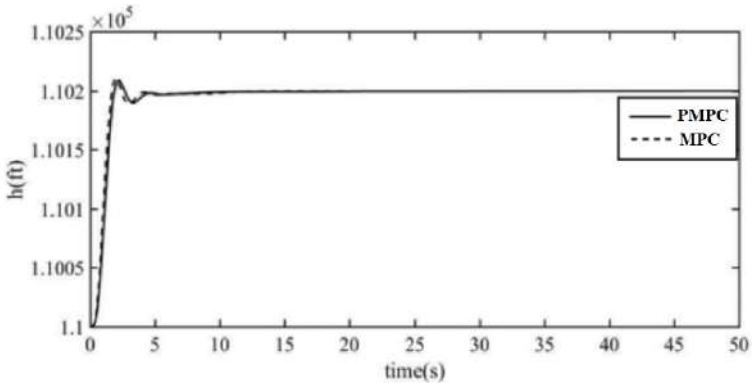

Figure 6: Altitude response comparison.

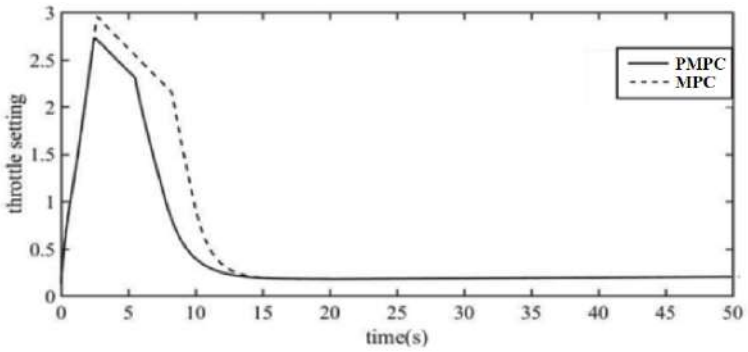

Figure 7: Throttle setting commands.

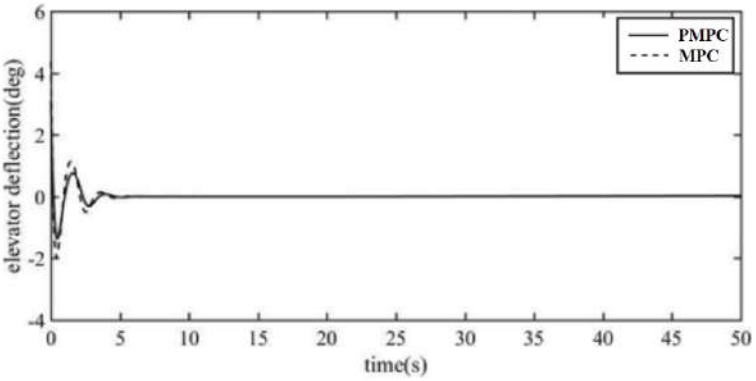

Figure 8: Control-surface deflection commands.

to the throttle setting, as shown in Figure **8**, the required deflection effort under PMPC is lower during the dynamic phase. To more clearly demonstrate the advantages of the proposed control method, numerical comparisons are presented below. For velocity tracking, throttle setting, and elevator deflection angle, the maximum values of the PMPC system are approximately 77.65%, 92.45%, and 65.48% of those of the MPC system, respectively.

From the above comparison, it can be concluded that the PMPC method combines the advantages of optimal preview and predictive control. It achieves improved tracking control of both flight velocity and altitude for the hypersonic vehicle, while also effectively reducing the control effort.

5. CONCLUSION

This study addresses the tracking control problem for hypersonic vehicles by integrating optimal preview control and predictive control to design a composite control system. The results demonstrate that the designed control system achieves satisfactory tracking performance for the hypersonic vehicle while satisfying the constraints on control inputs. Compared with

conventional model predictive control, the proposed method delivers superior dynamic performance and reduces the amplitude of control inputs, highlighting its advantages. This proposed method significantly enhances the precision and foresight of flight control by integrating two distinct control mechanisms. For intelligent aviation systems, it improves adaptive and collaborative decision-making capabilities. In terms of sustainable flight, it optimizes flight trajectories and energy consumption, reducing fuel usage and emissions, thereby advancing the development of greener aviation. Future work will apply the proposed method to flexible hypersonic vehicles to further validate its adaptability.

ACKNOWLEDGEMENTS

This work was supported by the National Natural Science Foundation of China, grant no. 62463017.

REFERENCE

[1] Tang W, Wang C, Shan L. Adaptive terminal sliding mode control of hypersonic vehicles based on ESO. Aircraft Engineering and Aerospace Technology 2025; 97(2): 247-259. https://doi.org/10.1108/AEAT-07-2024-0208

[2] Tang W, Jia C, Shi W. Fixed-time observer-based sliding mode control of air-breathing hypersonic vehicles subject to multisource uncertainties and actuator faults. Automatic Control and Computer Sciences 2025; 59(1): 78-90. https://doi.org/10.3103/S0146411625700075

[3] Yang W, Liang H, Sun C. Back-stepping robust control for a flexible air-breathing hypersonic vehicle using an α-filter-based uncertainty and disturbance estimator. International Journal of Control, Automation and Systems 2021; 19: 753-766. https://doi.org/10.1007/s12555-019-1034-0

[4] Xu BH, Wang DW, Zhang Y, Shi ZK. DOB-based neural control of flexible hypersonic flight vehicle considering wind effects. IEEE Transactions on Industrial Electronics 2017; 64: 8676-8685. https://doi.org/10.1109/TIE.2017.2703678

[5] Tarbouriech S, Turner M. Anti-windup design: an overview of some recent advances and open problems. IET Control Theory & Applications 2009; 3(1): 1-19. https://doi.org/10.1049/iet-cta:20070435

[6] Tang W, Long W, Gao H. Model predictive control of hypersonic vehicles accommodating constraints. IET Control Theory & Applications 2017; 11(15): 2599-2606. https://doi.org/10.1049/iet-cta.2017.0265

[7] Schwenzer M, Ay M, Bergs T. Review on model predictive control: An engineering perspective. The International Journal of Advanced Manufacturing Technology 2021; 117(5): 1327-1349. https://doi.org/10.1007/s00170-021-07682-3

[8] Morari M, Lee J H. Model predictive control: past, present and future. Computers & Chemical Engineering 1999; 23(4-5): 667-682. https://doi.org/10.1016/S0098-1354(98)00301-9

[9] Liu K, Hou Z, She Z. Reentry attitude tracking control for hypersonic vehicle with reaction control systems via improved model predictive control approach. Computer Modeling in Engineering & Sciences 2020; 122(1): 131-148. https://doi.org/10.32604/cmes.2020.08124

[10] Hu C, Yang X, Wei X. Robust model predictive control for hypersonic vehicle with state-dependent input constraints and parameter uncertainty. International Journal of Robust and Nonlinear Control 2021; 31(18): 9676-9691. https://doi.org/10.1002/rnc.5792

[11] Cui P, Gao C, An R. Fault-observer-based iterative learning model predictive controller for trajectory tracking of hypersonic vehicles. Journal of Systems Engineering and Electronics 2025; 36(3): 803-813. https://doi.org/10.23919/JSEE.2025.000033

[12] Yang X, Lv W, Hu C. Tube-model predictive control based on sum of squares for hypersonic vehicle with state-dependent input constraints. Transactions of the Institute of Measurement and Control 2022; 44(5): 1000-1013. https://doi.org/10.1177/01423312211046504

[13] Birla N, Swarup A. Optimal preview control: A review. Optimal Control Applications and Methods 2015; 36(2): 241-268. https://doi.org/10.1002/oca.2106

[14] Lu Y, Zhang X, Wang Z. Optimal containment preview control for continuous-time multi-agent systems using internal model principle. International Journal of Systems Science 2023; 54(4): 802-821. https://doi.org/10.1080/00207721.2022.2146987

[15] Xu H, Mirmirani M D, Ioannou P A. Adaptive sliding mode control design for a hypersonic flight vehicle. Journal of Guidance, Control, and Dynamics 2004; 27(5): 829-838. https://doi.org/10.2514/1.12596

Received on 19-11-2025 Accepted on 17-12-2025 Published on 31-12-2025

© 2025 Liu *et al*.
This is an open access article licensed under the terms of the Creative Commons Attribution License (http://creativecommons.org/licenses/by/4.0/) which permits unrestricted use, distribution and reproduction in any medium, provided the work is properly cited.